

# Molecular mechanisms driving the microgels behaviour: a Raman spectroscopy and Dynamic Light Scattering study

Valentina Nigro<sup>a,b</sup>, Francesca Ripanti<sup>b,\*</sup>, Roberta Angelini<sup>a,b,\*</sup>, Angelo Sarra<sup>c</sup>, Monica Bertoldo<sup>d</sup>, Elena Buratti<sup>e</sup>, Paolo Postorino<sup>b,\*</sup>, Barbara Ruzicka<sup>a,b</sup>

<sup>a</sup>*Istituto dei Sistemi Complessi del Consiglio Nazionale delle Ricerche (ISC-CNR), sede Sapienza, P.z.le Aldo Moro 5, I-00185 Roma, Italy*

<sup>b</sup>*Dipartimento di Fisica, Sapienza Università di Roma, P.le Aldo Moro 5, 00185 Roma, Italy*

<sup>c</sup>*Dipartimento di Scienze, Università degli Studi Roma Tre, via della Vasca Navale 84, 00146 Roma, Italy*

<sup>d</sup>*Istituto per la Sintesi Organica e la Fotoreattività del Consiglio Nazionale delle Ricerche (ISOF-CNR), via P. Gobetti 101, 40129 Bologna, Italy*

<sup>e</sup>*Istituto per i Processi Chimico-Fisici del Consiglio Nazionale delle Ricerche (IPCF-CNR), Area della Ricerca, Via G.Moruzzi 1, I-56124 Pisa, Italy*

---

## Abstract

Responsive microgels based on poly(N-isopropylacrylamide) (PNIPAM) exhibit peculiar behaviours due to the competition between the hydrophilic and hydrophobic interactions of the constituent networks. The interpenetration of poly-acrylic acid (PAAc), a pH-sensitive polymer, within the PNIPAM network, to form Interpenetrated Polymer Network (IPN) microgels, affects this delicate balance and the typical Volume-Phase Transition (VPT) leading to complex behaviours whose molecular nature is still completely unexplored.

Here we investigate the molecular mechanism driving the VPT and its influence on particle aggregation for PNIPAM/PAAc IPN microgels by the joint use of Dynamic Light Scattering and Raman Spectroscopy. Our results highlight that PNIPAM hydrophobicity is enhanced by the interpenetration of PAAc promoting inter-particle interactions, a crossover concentration is found above which aggregation phenomena become relevant. Moreover we find that, at variance with PNIPAM, for IPN microgels a double-step molecular mechanisms occurs upon crossing the VPT, the first involving the coil-to-globule transition typical of PNIPAM and the latter associated to PAAc steric hindrance.

**Keywords:** Microgels - Swelling behaviour - Raman Spectroscopy - Dynamic Light Scattering

---

## 1. Introduction

Responsive microgels are highly attractive systems for several technological applications due to their high responsiveness to slight changes of environmental conditions [1]. Smart microgels have indeed many applications in agriculture, construction, cosmetics and pharmaceuticals industries, in artificial organs, and tissue engineering

---

\*Corresponding authors: francesca.ripanti@uniroma1.it (F.Ripanti); roberta.angelini@roma1.infn.it (R.Angelini); paolo.postorino@roma1.infn.it (P.Postorino)

[2–7]. Moreover they are widely investigated in fundamental physics as good model systems for understanding the intriguing behaviours of soft colloids [8–10]. Their interparticle potential and their effective volume fraction can be indeed modulated through easily accessible control parameters driving the system to unconventional phase-behaviours [11–14], drastically different from those of conventional hard colloidal systems [15–22].

In the last years, poly(N-isopropylacrylamide) (PNIPAM) has become very popular due to its thermo-sensitivity [23]: at room temperature the polymer is hydrophilic and strongly hydrated in solution, while it becomes hydrophobic above 305 K, leading to a coil-to-globule transition that gives rise to a Volume-Phase Transition (VPT) from a swollen to a shrunken state [24] largely studied both experimentally [25–27] and theoretically [28–32]. The typical swelling/shrinking transition affects particle interactions and drives the system towards unusual phase behaviours [1, 11, 12, 33, 34], controlled by changing concentration [11, 35], solvents [36], internal structure and composition (such as number and distribution of cross-linking points [27, 37] and core-shell structure [38, 39]) or by introducing additives into the PNIPAM network [38].

This mechanism can be even more complex if pH-sensitive polymers are introduced within the PNIPAM network, allowing to tune the polymer/polymer and polymer/solvent interactions. In particular the introduction of poly-acrylic acid (PAAc) to the PNIPAM microgel permits to control the temperature dependence of the VPT by pH [40–45], PAAc content [46, 47] or ionic strength [40, 48]. The response of PNIPAM-PAAc microgels is strictly related to the mutual interference between the two monomers (Fig. 1) [39–41, 43, 48–51]. If the PAAc is interpenetrated into PNIPAM to obtain PNIPAM/PAAc Interpenetrated Polymer Network (IPN) microgel, [42, 46, 52–55] the coil-to-globule transition temperature of PNIPAM is almost unchanged [47], since irreversible chemical bonds between PNIPAM and PAAc chains are mainly excluded. This leaves the VPT temperature almost the same for PNIPAM and IPN microgels. Up to now a microscopic interpretation of the swelling behaviour for linear PNIPAM derives from the Flory Rehner theory that recently applied to PNIPAM based microgel under proper approximations [25, 56]. However, despite the numerous investigations on the VPT of PNIPAM microgels, a clear picture of the molecular mechanism behind swelling is still missing. To this aim Raman spectroscopy represents a powerful tool to highlight molecular changes related to the swelling behaviour as previously reported for linear PNIPAM [57, 58] and PNIPAM microgels [59, 60]. The main outcomes of these investigations underline that the principal groups involved in the swelling are the CH<sub>2</sub> stretching bands of the methylene group and the CH<sub>3</sub> stretching bands of the isopropyl group (Fig. 1). In the case of IPN microgels the presence of PAAc leads to more complex behaviour whose molecular nature has never been investigated up to now.

In the present work we report on a careful study for PNIPAM and IPN microgels combining Dynamic Light Scattering (DLS) and Raman spectroscopy. The interpretation of the experimental results allowed us to

recognize different microscopic behaviours for the two systems. In particular, at variance with PNIPAM, we identify two molecular mechanisms driving the volume phase transition: one responsible for the coil-to-globule transition of the PNIPAM and the other ascribed to the PAAc steric hindrance.

## 2. Experimental Methods

### 2.1. Sample preparation

**Materials** N-isopropylacrylamide (NIPAM) (Sigma-Aldrich), purity 97 %, and N,N'-methylene-bis-acrylamide (BIS) (Eastman Kodak), electrophoresis grade, were purified by recrystallization from hexane and methanol, respectively, dried under reduced pressure (0.01 mmHg) at room temperature and stored at 253 K. Acrylic acid (AAc) (Sigma-Aldrich), , purity 99 %, with 180 - 220 ppm of MEHQ as inhibitor, was purified by distillation (40 mmHg, 337 K) under nitrogen atmosphere on hydroquinone and stored at 253 K. Sodium dodecyl sulphate (SDS), purity 98 %, potassium persulfate (KPS), purity 98 %, ammonium persulfate (APS), purity 98 %, N,N,N',N'-tetramethylethylenediamine (TEMED), purity 99 %, ethylenediaminetetraacetic acid (EDTA), purity  $\geq 98.5$  %,  $\text{NaHCO}_3$ , purity 99.7 - 100.3 % were all purchased from Sigma-Aldrich and used as received. Ultrapure water (resistivity:  $18.2 \text{ M}\Omega \cdot \text{cm}$  at 298 K) was obtained with Millipore Direct-Q<sup>®</sup> 3 UV purification system. All other solvents were RP grade (Sigma Aldrich) and were used as received. Before use, dialysis tubing cellulose membrane, cut-off 14,000 Da, from Sigma-Aldrich, was washed for 3 h in running distilled water, treated at 343 K for 10 min into a solution containing a 3.0 % weight concentration of  $\text{NaHCO}_3$  and 0.4 % of EDTA, rinsed in distilled water at 343 K for 10 min and finally in fresh distilled water at room temperature for 2 h.

**Synthesis of PNIPAM and IPN microgels** PNIPAM micro-particles were synthesized by precipitation polymerization with  $(24.162 \pm 0.001)$  g of NIPAM,  $(0.4480 \pm 0.0001)$  g of BIS and  $(3.5190 \pm 0.0001)$  g of SDS solubilized in 1560 mL of ultrapure water and transferred into a 2000 mL four-necked jacketed reactor equipped with condenser and mechanical stirrer. The solution was deoxygenated by bubbling nitrogen inside for 1 h and then heated at  $(343.0 \pm 0.1)$  K.  $(1.0376 \pm 0.0001)$  g of KPS (dissolved in 20 mL of deoxygenated water) was added to initiate the polymerization and the reaction was allowed to proceed for 16 h. The resultant PNIPAM microgel was purified by dialysis against distilled water with frequent water change for 2 weeks. In the second step IPN microgels were synthesized by a sequential free radical polymerization method [42] with  $(140.08 \pm 0.01)$  g of the PNIPAM dispersion at the final weight concentration of 1.06 %. 5 mL of AAc was copolymerized with  $(1.1081 \pm 0.0001)$  g of BIS into the preformed PNIPAM microparticles at temperature in the range  $293 \div 295$  K, where PNIPAM particles are swollen allowing the growth of the PAAc network inside

them. The mixture was diluted with ultrapure water up to a volume of 1260 mL and transferred into a 2000 mL four-necked jacketed reactor kept at  $(294 \pm 1)$  K by circulating water and deoxygenated by bubbling nitrogen inside for 1 h. 0.56 mL of TEMED were added and the polymerization was started with  $(0.4441 \pm 0.0001)$  g of ammonium persulfate and allowed to proceed for 4 h and 30 min. The obtained IPN microgel at the final PAAc concentration of  $C_{PAAc} = 23\%$  was purified by dialysis against distilled water with frequent water change for 2 weeks and then lyophilized up to 1.00 % weight concentration. Samples at different weight concentrations, in the following referred as  $C_w$ , were obtained by dilution in  $H_2O$ .

## 2.2. Dynamic Light Scattering

Dynamic Light Scattering measurements have been performed with a light scattering setup, where a monochromatic and polarized beam emitted from a solid state laser (100 mW at  $\lambda=642$  nm) is focused on the sample placed in a cylindrical VAT for index matching and temperature control. The scattered intensity is collected by single mode optical fibers at fixed scattering angles, namely  $\theta=90^\circ$ , corresponding to  $Q = 0.018 \text{ nm}^{-1}$ , according to the relation  $Q=(4\pi n/\lambda) \sin(\theta/2)$ . The information on the system dynamics are extrapolated from the normalized intensity autocorrelation function  $g_2(Q, t) = \langle I(Q, t)I(Q, 0) \rangle / \langle I(Q, 0) \rangle^2$ , directly measured through DLS with a high coherence factor close to the ideal unit value. Measurements have been performed on aqueous suspensions of PNIPAM and IPN microgels at fixed PAAc content ( $C_{PAAc} = 23\%$ ) as a function of temperature in the range  $T=(293 \div 313)$  K, at four weight concentrations ( $C_w=0.1\%$ ,  $C_w=0.3\%$ ,  $C_w=0.5\%$  and  $C_w=0.8\%$ ) and pH 5.5. Reproducibility has been tested by repeating measurements several times.

As usual for colloidal systems, the intensity correlation functions are well described by the Kohlrausch-Williams-Watts expression [61, 62]:

$$g_2(Q, t) = 1 + b[(e^{-t/\tau})^\beta]^2 \quad (1)$$

where  $b$  is the coherence factor,  $\tau$  is an "effective" relaxation time, defining the decay constant  $\Gamma(Q) = 1/\tau(Q)$ , and  $\beta$  describes the deviation from the simple exponential decay ( $\beta = 1$ ) usually found in monodisperse systems and gives a measurement of the relaxation times distribution due to the intrinsic sample polydispersity. Many glassy materials show a stretching of the correlation functions (here referred to as "stretched behaviour") characterized by an exponent  $\beta < 1$ . Hydrodynamic radii  $R_H$  have been determined from the decay constant  $\Gamma(Q) = Dq^2$  obtained through the analysis of the intensity correlation functions  $g_2(Q, t)$  in the high dilution limit ( $C_w=0.1\%$ ).

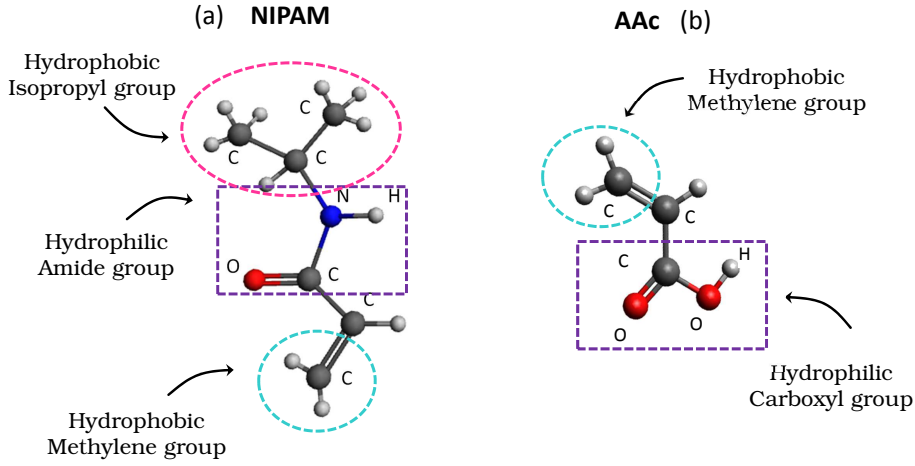


Figure 1: Sketch of (a) NIPAM and (b) AAc molecular structure.

### 2.3. Raman Spectroscopy

Raman measurements have been carried out using a Horiba HR-Evolution microspectrometer in backscattering geometry, equipped with a He-Ne laser,  $\lambda = 632.8 \text{ nm}$  and  $30 \text{ mW}$  output power ( $\sim 15 \text{ mW}$  at the sample surface). The elastically scattered light was removed by a state-of-the-art optical filtering device based on three BraggGrate notch filters [63] which also allows to collect Raman spectra at very low frequencies (down to  $10 \text{ cm}^{-1}$  from the laser line). The detector was a Peltier-cooled charge-coupled device (CCD) and the resolution was better than  $3 \text{ cm}^{-1}$  thanks to a  $600 \text{ grooves/mm}$  grating with  $800 \text{ mm}$  focal length. The spectrometer was coupled with a confocal microscope supplied with a set of interchangeable objectives with long working distances and different magnifications ( $20\times - 0.35 \text{ NA}$  was used for the present experiment). Further details on the experimental apparatus can be found in [64]. Measurements have been performed on aqueous suspensions of PNIPAM and IPN microgels at fixed PAAc concentration ( $C_{PAAc}=23 \%$ ) in the temperature range  $T=(293\div 313) \text{ K}$  across the VPT, at two weight concentrations ( $C_w=0.3 \%$  and  $C_w=5.0 \%$ ) and pH 5.5. Note that several measurements have been performed at lower weight concentrations resulting in a low signal-to-noise ratio that gives origin to misleading determination of the peak frequency.

## 3. Results and Discussions

In order to connect the dynamical response to molecular changes of PNIPAM and IPN microgels across the VPT, we combine Dynamic Light Scattering and Raman spectroscopy measurements.

The relaxation time and the stretching parameter for both PNIPAM and IPN microgels are reported in Fig.2 as a function of temperature at four weight concentrations ( $C_w=0.1 \%$ ,  $C_w=0.3 \%$ ,  $C_w=0.5 \%$  and  $C_w=0.8 \%$ ) as obtained by fitting the  $g_2(Q, t)$  with Eq.(1). In the case of pure PNIPAM (Fig.2(a)) the well known dynamical

transition associated to the VPT is evidenced [25, 44]: as temperature increases, the relaxation time  $\tau$  slightly decreases up to the volume phase transition temperature (VPTT), above which it decreases to its lowest value, corresponding to the shrunken state and indicating a fastening of the dynamics related to the reduced size of particles.

In the case of IPN microgels a different scenario shows up (Fig.2(b)) and the temperature dependence of the relaxation time above the VPTT is strongly affected by weight concentration: while at low  $C_w$  it is similar to that of pure PNIPAM, for  $C_w \geq 0.3\%$  it is reversed. The sudden increase above the VPTT indicate a slowing down of the dynamics and the formation of aggregates. The presence of PAAc, in fact, affects the delicate balance between hydrophobic and hydrophilic interactions. In particular, at this pH conditions (pH 5.5), where the fraction of deprotonated AAc moieties ( $\text{COO}^-$ , Fig.1(b)) is small but not negligible, the collapse of the PNIPAM network above the VPTT is supposed to favor the exposure of PAAc dangling chains and in turn interparticle interactions. The dynamical transition associated to the VPT is also observed in the temperature behaviour of the stretching parameter  $\beta$  for PNIPAM and IPN microgels reported in Fig.2(c),(d). Moreover in the case of IPN intriguing differences depending on concentration are observed: for  $C_w < 0.3\%$   $\beta$  decreases upon crossing the VPTT, while for  $C_w \geq 0.3\%$  microgel collapse leads to an increase of the stretching coefficient that gets more pronounced with increasing concentration. Both  $\tau$  and  $\beta$  behaviours sign the existence of a crossover concentration  $C_w = 0.3\%$  in IPN microgels at  $C_{PAAc} = 23\%$  above which interparticle interactions become important giving rise to aggregation.

To deeply investigate the molecular mechanism driving the VPT and the conformational changes induced by microgel collapse, Dynamic Light Scattering measurements have been complemented with Raman spectroscopy on PNIPAM and IPN microgels at weight concentration equal and above the critical value  $C_w = 0.3\%$ . Raman spectra over the frequency range from 800 to 3000  $\text{cm}^{-1}$  for both PNIPAM and IPN microgels are reported in Fig.3 together with the assignment of the principal vibrational modes. Interestingly the spectra are dominated by the contribution associated to the C-C and C-H vibration bands, mainly derived from NIPAM (Fig.1(a)).

To investigate the molecular changes induced by temperature across the VPT, we focus our attention on the spectral range between 2850  $\text{cm}^{-1}$  and 3000  $\text{cm}^{-1}$ , where bands ascribed to vibrations of  $\text{CH}_2$  (methylene group, Fig.1(a)(b)) and  $\text{CH}_3$  (in isopropyl group, Fig.1(a)) are present. As recently observed in PNIPAM [60], changes of these bands, sensitive to hydrogen bond variations, are related to different interactions both among polymers and between polymer side groups and water molecules surrounding them. Raman spectra of PNIPAM and IPN microgels at two concentrations  $C_w = 0.3\%$  (critical concentration) and  $C_w = 5.0\%$  are reported in Fig.4 at temperatures  $T = 297\text{ K}$  and  $T = 316\text{ K}$ , below and above the VPTT (Fig.4(a,b,c,d)). The entire temperature

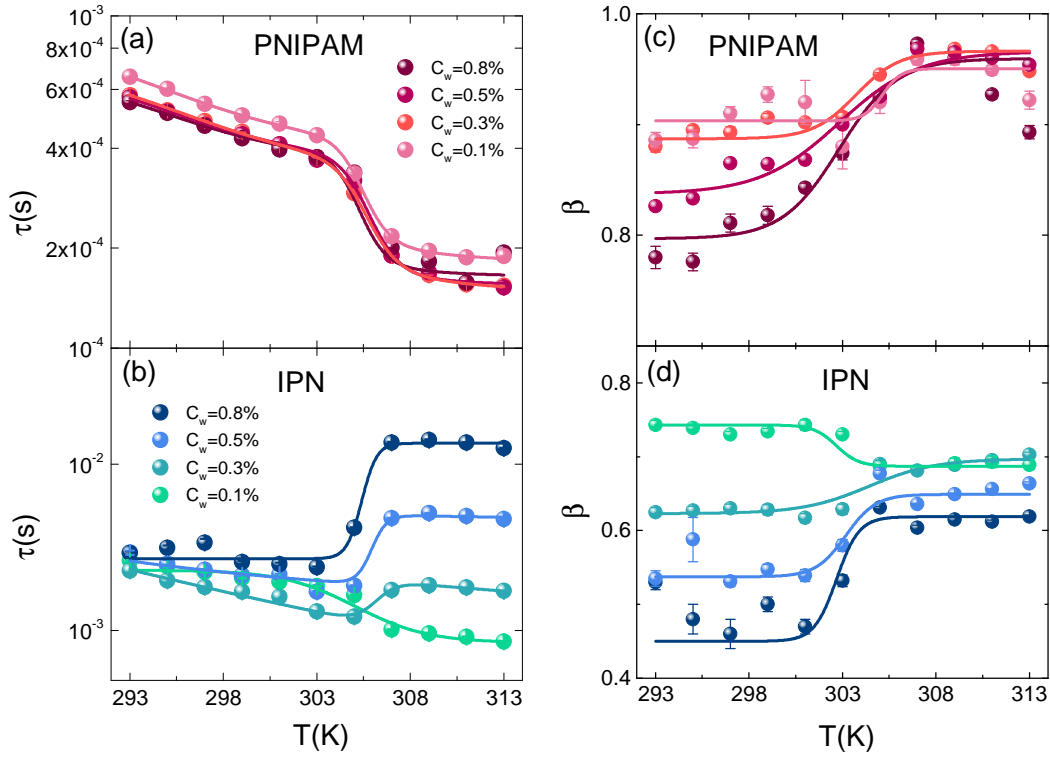


Figure 2: (a,b) Relaxation time and (c,d) shape parameter as a function of temperature for PNIPAM and IPN microgels at  $C_{PAAc}=23\%$  at the indicated weight concentrations. Solid lines are guides to eyes.

behaviour upon crossing the VPT is reported in Fig.4(e) for IPN microgels at  $C_w=5.0\%$  as an example. Spectra have been deconvolved by four Gaussian contributions (Fig.4(e)) that have been assigned to different C-H stretching of the NIPAM molecule in the hydrated state ( $T=297\text{ K}$ ), according to previous works in literature [57, 65]: symmetric stretching of  $\text{CH}_3$  ( $2880\text{ cm}^{-1}$ ), symmetric and antisymmetric stretching of  $\text{CH}_2$  ( $2920\text{ cm}^{-1}$ ,  $2945\text{ cm}^{-1}$  respectively), antisymmetric stretching of  $\text{CH}_3$  ( $2988\text{ cm}^{-1}$ ).

Looking at Fig.4(a) and Fig.4(b), we notice a significant transfer of the spectral weight between the two central peaks ascribed to symmetric and antisymmetric  $\text{CH}_2$  stretching modes of the methylene group. It is well known that the intensity ratio between the symmetric and antisymmetric stretching modes (lower and higher frequency, respectively) is related to the lateral packing density of any polymer chain [66], in particular an increase of their ratio implies the folding of the linear chain. Therefore in our case the increase of the intensity ratio upon crossing the VPTT in both PNIPAM and IPN microgels (Fig.4(a,b,c,d)) can be ascribed to an increase of the packing density due to the coil-to-globule transition of PNIPAM signaling that their shrinking still drives the molecular changes across the VPT even when the PAAc is interpenetrated within the PNIPAM network.

Additional information on the swelling behaviour can be gained from the temperature dependence of the

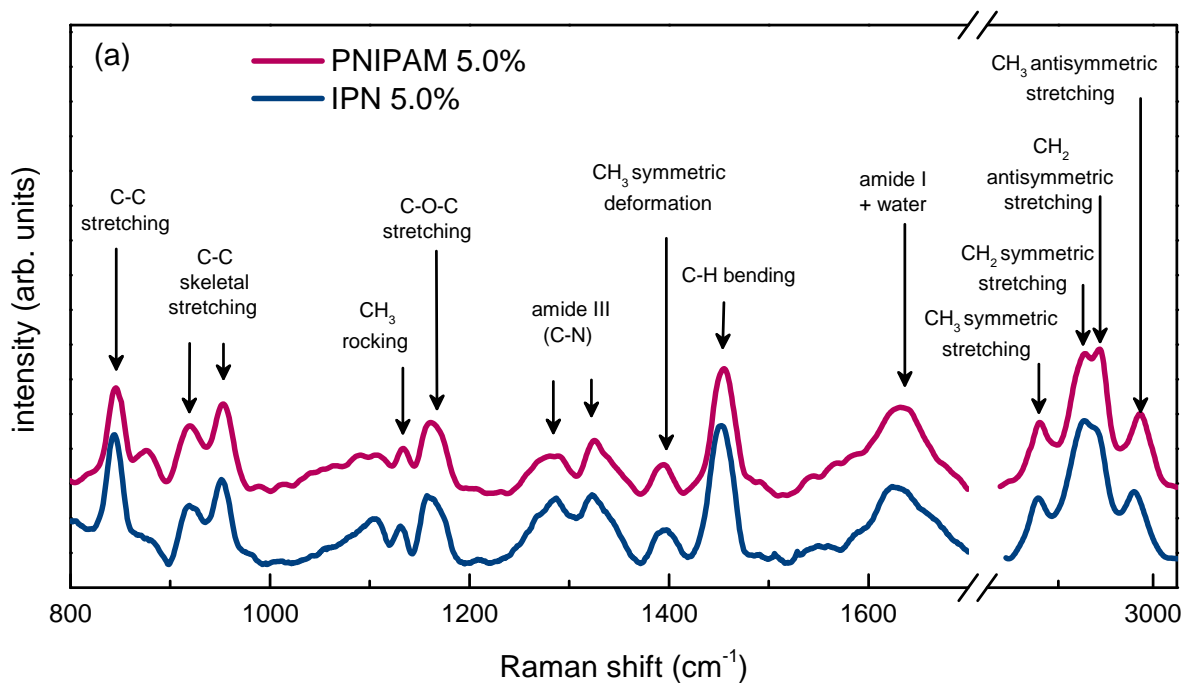


Figure 3: Raman spectra for PNIPAM and IPN microgels at fixed temperature ( $T=316$  K) and concentration ( $C_w=5.0$  %).

antisymmetric  $\text{CH}_3$  stretching (higher frequency peak at  $2988\text{ cm}^{-1}$ ) [57]. A clear frequency red-shift upon crossing the VPTT is observed. This downshift with temperature (Fig.4) is the main signature of the dehydration of the isopropyl group of NIPAM (Fig.1(a)). In fact, as previously observed and theoretically investigated, the higher number of water molecules surrounding the  $\text{CH}_3$  groups correlates with the higher frequency of the  $\text{CH}_3$  stretching vibration [67, 68]. The frequency peak for PNIPAM microgels at  $C_w=0.3$  % is reported in Fig.5(a) as a function of temperature and compared with the hydrodynamic radius  $R_H$  obtained from DLS. Both quantities show actually an identical temperature behaviour: they monotonically decrease as temperature increases showing a sharp transition close to the VPTT. This behaviour endorses the idea that the volume phase transition is accompanied by a reorganization of the neighboring water molecules leading to significant decrease of the hydration of the methyl group.

For IPN microgels the scenario is more complex since the presence of PAAc affects the balance between hydrophilic and hydrophobic interactions and the net charge. The decrease with temperature of the  $\text{CH}_3$  frequency and of the hydrodynamic radius  $R_H$ , reported in Fig.5(b) for IPN microgels at  $C_w=0.3$  %, confirms that the main features of the coil-to-globule transition of PNIPAM are preserved. Moreover the smoother decrease with respect to PNIPAM is accompanied by an additional bump upon crossing the VPTT, suggesting the presence of additional molecular mechanisms due to the interpenetration of PAAc network. This two-steps decay can be explained in terms of a reduced hydration of the isopropyl groups of NIPAM (first drop) accompanied



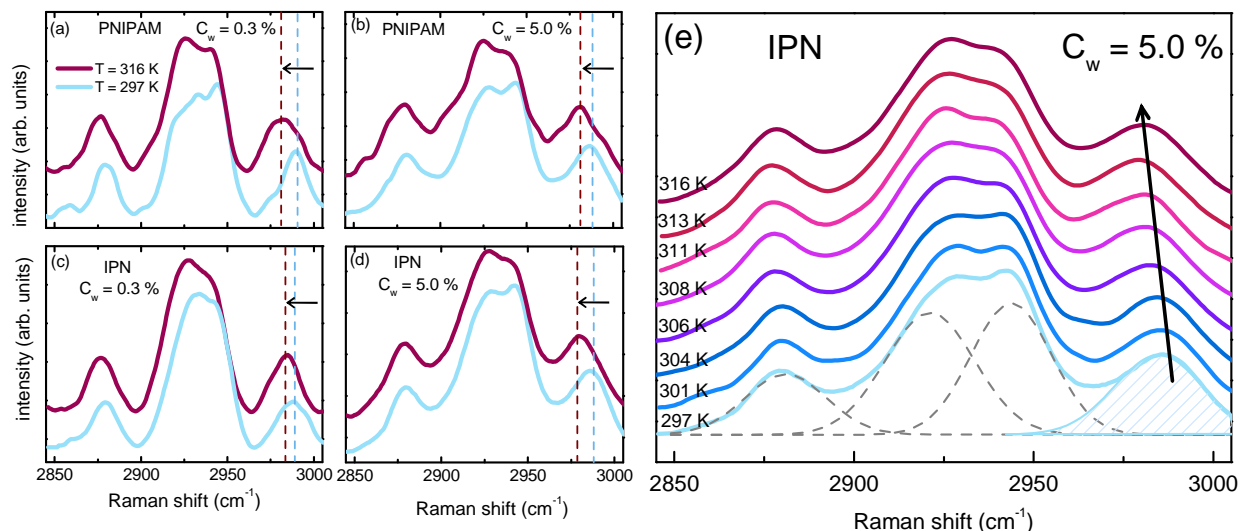


Figure 4: Raman spectra for (a)(b) PNIPAM and (c)(d) IPN microgels at temperature below (light cyan) and above (red) the VPTT, at  $C_w=0.3\%$  and  $C_w=5.0\%$ . (e) Raman spectra for IPN microgels at  $C_w=5.0\%$  at the indicated temperatures. Four Gaussian contributions are reported as discussed in the text. Dashed lines and arrows highlight the frequency of  $\text{CH}_3$  stretching band.

by a new mechanism (bump) due to the presence of PAAc that with its steric hindrance limits the microgel shrinking.

The behaviours of the  $\text{CH}_3$  stretching frequency  $\nu(T)$  for PNIPAM and IPN microgels at two concentrations ( $C_w=0.3\%$  and  $C_w=5.0\%$ ) are reported in Fig.6(a) and Fig.6(b), respectively. The decrease of the frequency at higher concentration indicates a reduction of water molecules surrounding the isopropyl group corresponding to an higher internal packing density. For IPN microgels (Fig.6(b)) the bump above mentioned becomes more evident at higher concentration ( $C_w=5.0\%$ ), suggesting that the C-H bonds of the PNIPAM methyl groups get stronger as particles become closer.

A comparison between Fig.6(a) and Fig.6(b) highlights that for  $C_w=0.3\%$  lower values of  $\text{CH}_3$  frequency are observed in IPN with respect to PNIPAM microgels with a consequent smaller number of water molecules surrounding the PNIPAM side chains ( $\text{CH}_3$  groups) in IPN and an higher internal packing density that we attribute to the interpenetration of the PAAc network. These results suggest that most of the differences between PNIPAM and IPN microgels are strictly related to the combined effect of reduced hydration of the  $\text{CH}_3$  groups of PNIPAM and to the topological rearrangements of the polymer networks within the microgel particle. Interpenetrating PAAc within PNIPAM enhances the hydrophobicity of the microgel particles perturbing the role played by water molecules. At these pH conditions (pH 5.5) the intra-particle and inter-particle interactions between CONH (PNIPAM) and COOH (PAAc) groups make respectively IPN microgel more hydrophobic and favor aggregation. The same comparison for  $C_w=5.0\%$  (Fig.6(a) and Fig.6(b)) evidences that the initial and

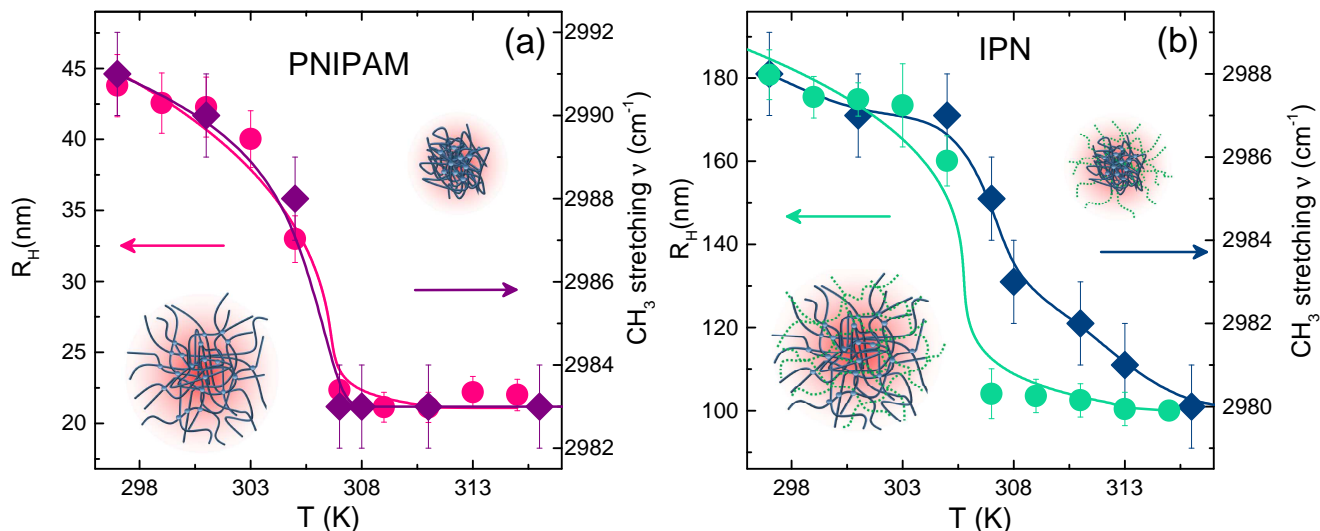


Figure 5: Hydrodynamic radius  $R_H$  and  $\text{CH}_3$  frequency as a function of temperature for (a) PNIPAM and (b) IPN microgels at low concentrations. Magenta and green solid lines are the fit of  $R_H(T)$  through the Flory-Rehner theory, purple and blue solid lines are guide to eyes for the  $\text{CH}_3$  frequency behaviour.

final values of the frequency are not significantly different for PNIPAM and IPN microgels indicating that for this concentration a dehydration limit has been reached independently of the system.

In summary, for PNIPAM microgel the VPT is characterized by a decrease of the relaxation time (Fig.2(a)) and of the  $\text{CH}_3$  frequency (Fig.5(a)) that reflect the rearrangement of water molecules as expected for swelling phenomenon. In the case of IPN microgel for  $C_w \geq 0.3\%$  the increase of the relaxation time above the VPTT (Fig.2(b)), ascribed to aggregation phenomena, is associated to a more hydrophobic nature with respect to pure PNIPAM microgels, as also reflected in the temperature dependence of  $\text{CH}_3$  frequency (Fig.5(b) and Fig.6(b)). Therefore we can argue that this novel feature can be considered a distinctive signature of IPN microgels.

## 4. Conclusions

The temperature behaviour across the VPT in PNIPAM and IPN microgels has been investigated through DLS and Raman spectroscopy. DLS has provided direct information about the hydrodynamic radius behaviour from a swollen to a shrunken state, whereas Raman spectroscopy has allowed to detect molecular modifications upon crossing the VPT not detectable through DLS. Surprisingly, for PNIPAM microgels, DLS and Raman spectroscopy yield equivalent temperature behaviours of completely different physical quantities. At variance with PNIPAM, in IPN microgels the fingerprints of two different microscopic mechanisms are recognized. The first is similar to pure PNIPAM microgel: when the microgel particle goes towards the shrunken state, the number of water molecules surrounding the methyl group is reduced and the frequency of  $\text{CH}_3$  stretching

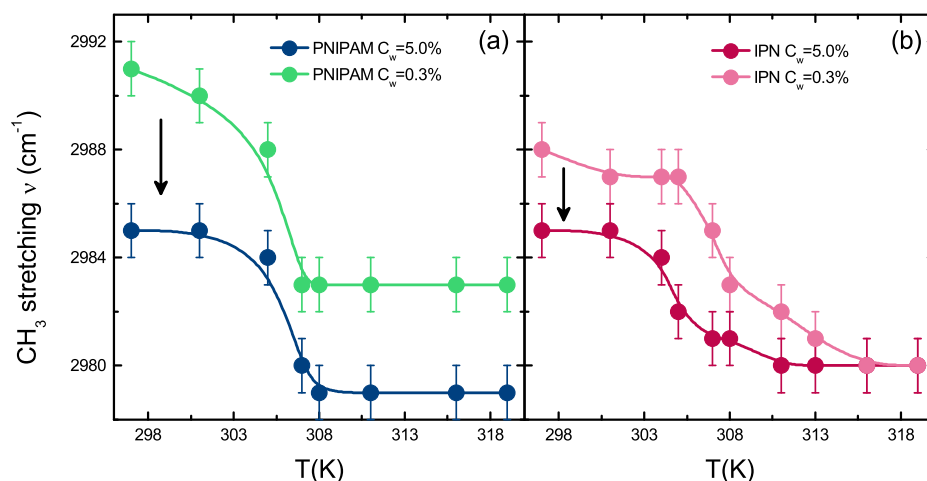


Figure 6:  $\text{CH}_3$  frequency as a function of temperature for (a) PNIPAM and (b) IPN microgels at  $C_w=0.3\%$  and  $C_w=5.0\%$ . Solid lines are guides to eyes. The arrows underline the reduction of  $\text{CH}_3$  frequency on increasing microgel concentration.

abruptly decreases. The latter is evidenced by an additional bump in the temperature dependence of the  $\text{CH}_3$  frequency. This behaviour is peculiar of IPN microgel and is due to the presence of PAAc that enhances microgel hydrophobicity and limits the microgel shrinking.

Raman spectroscopy is therefore a particularly suitable probe for investigating the microscopic underlying interactions in these complex systems, showing that hydrophobicity plays a crucial role not only in the swelling behaviour but also in the aggregation phenomena.

## Bibliography

## References

- [1] L. A. Lyon and A. Fernandez-Nieves. The Polymer/Colloid Duality of Microgel Suspensions. *Annu. Rev. Phys. Chem.*, 63:25–43, 2012.
- [2] S. V. Vinogradov. Colloidal microgels in drug delivery applications. *Curr. Pharm. Des.*, 12:4703–4712, 2006.
- [3] M. Das, H. Zhang, and E. Kumacheva. MICROGELS: Old Materials with New Applications. *Annu. Rev. Mater. Res.*, 36:117–142, 2006.
- [4] J. S. Park, H. N. Yang, D. G. Woo, S. Y. Jeon, and K. H. Park. Poly(N-isopropylacrylamide-co-acrylic acid) nanogels for tracing and delivering genes to human mesenchymal stem cells. *Biomaterials*, 34:8819–8834, 2013.

- [5] M. Hamidi, A. Azadi, and P. Rafie. Hydrogel nanoparticles in drug delivery. *Adv. Drug Deliv. Rev.*, 60:1638–1649, 2008.
- [6] N. M. B. Smeets and T. Hoare. Designing Responsive Microgels for Drug Delivery Applications. *J. Polym. Sci. A Polym. Chem.*, 51:3027–3043, 2013.
- [7] S. Su, Ali Md. Monsur, C. D. M. Filipe, Y. Li, and R. H. Pelton. Microgel-Based Inks for Paper-Supported Biosensing Applications. *Biomacromolecules*, 9:935–941, 2008.
- [8] C. N. Likos, N. Hoffmann, H. Löwen, and A. A. Louis. Exotic fluids and crystals of soft polymeric colloids. *J. Phys. Cond. Matter*, 14:7681–7698, 2002.
- [9] P. E. Ramírez-González and M. Medina-Noyola. Glass transition in soft-sphere dispersions. *Journal of Physics: Condensed Matter*, 21(7):075101–13, 2009.
- [10] D.M. Heyes and A.C.Branka. Interactions between microgel particles. *Soft Matter*, 5:2681, 2009.
- [11] H. Wang, X. Wu, Z. Zhu, C. S. Liu, and Z. Zhang. Revisit to phase diagram of poly(N-isopropylacrylamide) microgel suspensions by mechanical spectroscopy. *J. Chem. Phys.*, 140:024908, 2014.
- [12] P. S. Mohanty, D. Paloli, J. J. Crassous, E. Zaccarelli, and P. Schurtenberger. Effective interactions between soft-repulsive colloids: Experiments, theory and simulations. *J. Chem. Phys.*, 140:094901, 2014.
- [13] T. Hellweg, C.D. Dewhurst, E. Brückner, K.Kratz, and W.Eimer. Colloidal crystals made of poly(N-isopropylacrylamide) microgel particles. *Colloid. Polym. Sci.*, 278:972–978, 2000.
- [14] J. Wu, B. Zhou, and Z. Hu. Phase behavior of thermally responsive microgel colloids. *Phys. Rev. Lett.*, 90(4):048304–4, 2003.
- [15] P. N. Pusey and W. van Megen. Phase behaviour of concentrated suspensions of nearly hard colloidal spheres. *Nature*, 320:340–342, 1986.
- [16] A. Imhof and J. K. G. Dhont. Experimental Phase Diagram of a Binary Colloidal Hard-Sphere Mixture with a Large Size Ratio. *Phys. Rev. Lett.*, 75:1662–1665, 1995.
- [17] K. N. Pham, A. M. Puertas, J. Bergenholtz, S. U. Egelhaaf, A. Moussaïd, P. N. Pusey, A. B. Schofield, M. E. Cates, M. Fuchs, and W. C. K. Poon. Multiple Glassy States in a Simple Model System. *Science*, 296:104–106, 2002.

- [18] T. Eckert and E. Bartsch. Re-entrant glass transition in a colloid-polymer mixture with depletion attractions. *Phys. Rev. Lett.*, 89:125701–4, 2002.
- [19] P. J. Lu, E. Zaccarelli, F. Ciulla, A. B. Schofield, F. Sciortino, and D. A. Weitz. Gelation of particle with short range attraction. *Nature*, 453:499–503, 2008.
- [20] C. P. Royall, S. R. Williams, T. Ohtsuka, and H. Tanaka. Direct observation of a local structural mechanism for dynamical arrest. *Nat. Mater.*, 7:556–561, 2008.
- [21] B. Ruzicka, E. Zaccarelli, L. Zulian, R. Angelini, M. Sztucki, A. Moussaïd, T. Narayanan, and F. Sciortino. Observation of empty liquids and equilibrium gels in a colloidal clay. *Nat. Mater.*, 10:56–60, 2011.
- [22] R. Angelini, E. Zaccarelli, F. A. de Melo Marques, M. Sztucki, A. Fluerasu, G. Ruocco, and B. Ruzicka. Glass-glass transition during aging of a colloidal clay. *Nat. Commun.*, 5:4049–7, 2014.
- [23] R. H. Pelton and Chibante P. Preparation of aqueous lattices with N-isopropylacrylamide. *Colloids Surf.*, 20:247–256, 1986.
- [24] J. Wu, G. Huang, and Z. Hu. Interparticle Potential and the Phase Behavior of Temperature-Sensitive Microgel Dispersions. *Macromolecules*, 36:440–448, 2003.
- [25] V. Nigro, R. Angelini, M. Bertoldo, and B. Ruzicka. Swelling of responsive-microgels: experiments versus models. *Colloids Surf. A*, 532:389–396, 2017.
- [26] J. J. Lietor-Santos, B. Sierra-Martin, R. Vavrin, Z. Hu, U. Gasser, and A. Fernandez-Nieves. Deswelling Microgel Particles Using Hydrostatic Pressure. *Macromolecules*, 42:6225–6230, 2009.
- [27] K. Kratz, T. Hellweg, and W. Eimer. Structural changes in PNIPAM microgel particles as seen by SANS, DLS and EM techniques. *Polymer*, 42:6631–6639, 2001.
- [28] P.J. Flory. *Principles of Polymer Chemistry*. Cornell University, Ithaca, New York, 1953.
- [29] A.K. Lele, M.M. Hirve, M.V. Badiger, and R.A. Mashelkar. Predictions of bound water content in poly (N-isopropylacrylamide) gel. *Macromolecules*, 30:157–159, 1998.
- [30] T. Hino and J. M. Prausnitz. Swelling Equilibria for Heterogeneous Polyacrylamide Gels. *J. Appl. Polym. Sci*, 62:1635–1640, 1996.

- [31] K. Otake, H. Inomata, M. Konno, and S. Saito. Thermal-analysis of the volume phase-transition with N-Isopropylacrylamide gels. *Macromolecules*, 23:283–289, 1990.
- [32] T. Lòpez-Leòn and A. Fernandez-Nieves. Macroscopically probing the entropic influence of ions: deswelling neutral microgels with salt. *Phys. Rev. E*, 75:011801, 2007.
- [33] J. Mattsson, H. M. Wyss, A. Fernandez-Nieves, K. Miyazaki, Z. Hu, D. Reichman, and D. A. Weitz. Soft colloids make strong glasses. *Nature*, 462(5):83–86, 2009.
- [34] D. Paloli, P. S. Mohanty, J. J. Crassous, E. Zaccarelli, and P. Schurtenberger. Fluid–solid transitions in soft-repulsive colloids. *Soft Matter*, 9:3000–3004, 2013.
- [35] B. H. Tan, R. H. Pelton, and K. C. Tam. Microstructure and rheological properties of thermo-responsive poly(N-isopropylacrilamide) microgels. *Polymers*, 51:3238–3243, 2010.
- [36] P. W. Zhu and D. H. Napper. Light scattering studies of poly(N-isopropylacrylamide) microgel particle in mixed water-acetic acid solvents. *Macromol. Chem. Phys.*, 200:1950–1955, 1999.
- [37] K. Kratz and W. Eimer. Swelling Properties of Colloidal Poly(N-Isopropylacrylamide) Microgels in Solution. *Ber. Bunsenges. Phys. Chem.*, 102:848–854, 1998.
- [38] T. Hellweg, C. D. Dewhurst, W. Eimer, and K. Kratz. PNIPAM-co-polystyrene core-shell microgels: structure, swelling behavior, and crystallization. *Langmuir*, 20:4333–4335, 2004.
- [39] Z. Meng, J. K. Cho, S. Debord, V. Breedveld, and L. A. Lyon. Crystallization Behavior of Soft, Attractive Microgels. *J. Phys. Chem. B*, 111:6992–6997, 2007.
- [40] K. Kratz, T. Hellweg, and W. Eimer. Influence of charge density on the swelling of colloidal poly(N-isopropylacrylamide-co-acrylic acid) microgels. *Colloids Surf. A*, 170:137–149, 2000.
- [41] K. Kratz, T. Hellweg, and W. Eimer. Effect of connectivity and charge density on the swelling and local structure and dynamic properties of colloidal PNIPAM microgels. *Ber. Bunsenges. Phys. Chem.*, 102(11):1603–1608, 1998.
- [42] X. Xia and Z. Hu. Synthesis and Light Scattering Study of Microgels with Interpenetrating Polymer Networks. *Langmuir*, 20:2094–2098, 2004.
- [43] C. D. Jones and L. A. Lyon. Synthesis and Characterization of Multiresponsive Core-Shell Microgels. *Macromolecules*, 33:8301–8303, 2000.

- [44] V. Nigro, R. Angelini, M. Bertoldo, V. Castelvetro, G. Ruocco, and B. Ruzicka. Dynamic light scattering study of temperature and pH sensitive colloidal microgels. *J. Non-Cryst. Solids*, 407:361–366, 2015.
- [45] V. Nigro, R. Angelini, M. Bertoldo, F. Bruni, M.A. Ricci, and B. Ruzicka. Local structure of temperature and ph-sensitive colloidal microgels. *J. Chem. Phys.*, 143:114904–9, 2015.
- [46] Z. Hu and X. Xia. Hydrogel nanoparticle dispersions with inverse thermoreversible gelation. *Adv. Mater.*, 16(4):305–309, 2004.
- [47] J. Ma, B. Fan, B. Liang, and J. Xu. Synthesis and characterization of Poly(N-isopropylacrylamide)/Poly(acrylic acid) semi-IPN nanocomposite microgels. *J. Colloid Interface Sci.*, 341:88–93, 2010.
- [48] W. Xiong, X. Gao, Y. Zao, H. Xu, and X. Yang. The dual temperature/pH-sensitive multiphase behavior of poly(Nisopropylacrylamide-co-acrylic acid) microgels for potential application in *in situ* gelling system. *Colloids Surf. B: Biointerfaces*, 84:103–110, 2011.
- [49] L. A. Lyon, J. D. Debord, S. B. Debord, C. D. Jones, J. G. McGrath, and M. J. Serpe. Microgel Colloidal Crystals. *J. Phys. Chem. B*, 108:19099–19108, 2004.
- [50] P. Holmqvist, P. S. Mohanty, G. Nägele, P. Schurtenberger, and M. Heinen. Structure and Dynamics of Loosely Cross-Linked Ionic Microgel Dispersions in the Fluid Regime. *Phys. Rev. Lett.*, 109:048302–5, 2012.
- [51] S. B. Debord and L. A. Lyon. Influence of Particle Volume Fraction on Packing in Responsive Hydrogel Colloidal Crystals. *J. Phys. Chem. B*, 107:2927–2932, 2003.
- [52] X. Xia, Z. Hu, and M. Marquez. Physically bonded nanoparticle networks: a novel drug delivery system. *J. Control. Release*, 103:21–30, 2005.
- [53] J. Zhou, G. Wang, L. Zou, L. Tang, M. Marquez, and Z. Hu. Viscoelastic Behavior and In Vivo Release Study of Microgel Dispersions with Inverse Thermoreversible Gelation. *Biomacromolecules*, 9:142–148, 2008.
- [54] Z. Xing, C. Wang, J. Yan, L. Zhang, L. Li, and L. Zha. pH/temperature dual stimuli-responsive microcapsules with interpenetrating polymer network structure. *Colloid Polym. Sci.*, 288:1723–1729, 2010.

- [55] X. Liu, H. Guo, and L. Zha. Study of pH/temperature dual stimuli-responsive nanogels with interpenetrating polymer network structure. *Polymers*, 61(7):1144–1150, 2012.
- [56] M. Quesada-Pérez, J.A. Maroto-Centeno, J. Forcada, and R. Hidalgo-Alvarez. Gel swelling theories: the classical formalism and recent approaches. *Soft Matter*, 7:10536–10547, 2011.
- [57] J. Dybal, M. Trchova, and P. Schmidt. The role of water in structural changes of poly(n-isopropylacrylamide) and poly(n-isopropylmethacrylamide) studied by ftir, raman spectroscopy and quantum chemical calculations. *Vibrational Spectroscopy*, 51:44–51, 2009.
- [58] M.H. Futscher, M. Philipp, P. Müller-Buschbaum, and A. Schulte. The Role of Backbone Hydration of Poly(N-isopropyl acrylamide) Across the Volume Phase Transition Compared to its Monomer. *Scientific Reports*, 7(17012):1–10, 2017.
- [59] Z. Ahmed, E.A. Gooding, K.V. Pimenov, L. Wang, and S.A. Asher. Uv resonance raman determination of molecular mechanism of poly(n-isopropylacrylamide) volume phase transition. *J. Chem. Phys. B*, 113:4248–4256, 2009.
- [60] T. Wu, A.B. Zrimsek, S.V. Bykov, R.S. Jakubek, and S.A. Asher. Hydrophobic Collapse Initiates the Poly(N-isopropylacrylamide) Volume Phase Transition Reaction Coordinate. *The Journal of Physical Chemistry B*, 122(11):3008–3014, 2018.
- [61] R. Kohlrausch. Theorie des elektrischen rckstandes in der leidener flasche. *Annalen der Physik*, 2, 1854.
- [62] G. Williams and D. C. Watts. Non-Symmetrical Dielectric Relaxation Behavior Arising from a Simple Empirical Decay Function. *J. Chem. Soc. Faraday Trans.*, 66:80–85, 1970.
- [63] A.L. Glebov, O. Mokhun, A. Rapaport, S. Vergnole, V. Smirnov, and L. B. Glebov. Volume bragg gratings as ultra-narrow and multiband optical filters. *Proc. of SPIE*, 8428:84280C–4, 2012.
- [64] F. Capitani, S. Koval, R. Fittipaldi, S. Caramazza, E. Paris, W. S. Mohamed, J. Lorenzana, A. Nucara, L. Rocco, A. Vecchione, P. Postorino, and P. Calvani. Raman phonon spectrum of the Dzyaloshinskii-Moriya helimagnet  $Ba_2CuGe_2O_7$ . *Phys. Rev. B*, 91:214308, 2015.
- [65] Y. Tsuboi, M. Nishino, and N. Kitamura. Laser-induced reversible volume phase transition of a poly(n-isopropylacrylamide) gel explored by raman microspectroscopy. *Polymer Journal*, 40:367–374, 2008.



- [66] Y. Tsuboi, M. Nishino, and N. Kitamura. Laser-Induced Reversible Volume Phase Transition of a Poly(N-isopropylacrylamide) Gel Explored by Raman Microspectroscopy. *Polymer Journal*, 40(4):367–374, 2008.
- [67] P. Schmidt, J. Dybal, and M. Trchova. Investigations of the hydrophobic and hydrophilic interactions in polymer-water systems by atr ftir and raman spectroscopy. *Vibrational Spectroscopy*, 42:278–283, 2006.
- [68] P. Hobza and Z. Havlas. Improper, blue-shifting hydrogen bond. *Theoretical Chemistry Accounts*, 108(6):325–334, Dec 2002.